crystals

MDPI

Article

Understanding of Photophysical Processes in DIO Additive-Treated PTB7:$PC_{71}BM$ Solar Cells

Xiaojun Su [1,†], Rong Hu [2,*,†], Guanzhao Wen [3,†], Xianshao Zou [4], Mengyao Qing [3], Jun Peng [3], Xiaochuan He [5] and Wei Zhang [3,*]

1 Department of Basic Courses, Guangzhou Maritime University, Guangzhou 510725, China; suxiaojun@gzmtu.edu.cn
2 School of Materials Science and Engineering, Chongqing University of Arts and Sciences, Chongqing 402160, China
3 School of Physics and Materials Science, Guangzhou University, Guangzhou 510006, China; gzhwen@e.gzhu.edu.cn (G.W.); minnieq0808@gmail.com (M.Q.); speepengjun@gzhu.edu.cn (J.P.)
4 Division of Chemical Physics, Department of Chemistry, Lund University, 22100 Lund, Sweden; xianshao.zou@chemphys.lu.se
5 Songshan Lake Materials Laboratory, Dongguan 523808, China; hlcfreelook@gmail.com
* Correspondence: hurong_82@cqwu.edu.cn (R.H.); wzhang@gzhu.edu.cn (W.Z.)
† These authors contributed equally to this work.

Abstract: 1,8-diiodooctane (DIO) additive is an important method for optimizing the morphology and device performance of polythieno[3,4-b]-thiophene-co-benzodithiophene (PTB7)-based polymer solar cells. However, the effect of DIO additive on charge photogeneration dynamics of PTB7-based polymer solar cells is still poorly understood. In this work, the effect of DIO additive on the carrier photogeneration dynamics, as well as device performance of PTB7: [6,6]-phenyl-C_{71}-butyric acid methyl ester ($PC_{71}BM$) solar cells was studied. Bias-dependent photoluminescence (PL) experiments of a neat PTB7 device show that the exciton cannot be dissociated by the electric field in the device within the operating voltage range, but it can be effectively dissociated by the high electric field. PL and time-resolved PL studies show that DIO additive reduces the phase size of PTB7 in the blend film, resulting in an increased exciton dissociation efficiency. The carrier recombination processes were studied by transient absorption, which shows geminate carrier recombination was suppressed in the DIO-treated PTB7:$PC_{71}BM$ device in ultrafast time scale. The increased exciton dissociation efficiency and suppressed carrier recombination in ultrafast time scale play an important role for DIO-treated PTB7:$PC_{71}BM$ solar cells to attain a higher power conversion efficiency.

Keywords: polymer solar cells; PTB7:$PC_{71}BM$; DIO additive; carrier photogeneration

Citation: Su, X.; Hu, R.; Wen, G.; Zou, X.; Qing, M.; Peng, J.; He, X.; Zhang, W. Understanding of Photophysical Processes in DIO Additive-Treated PTB7:$PC_{71}BM$ Solar Cells. *Crystals* **2021**, *11*, 1139. https://doi.org/10.3390/cryst11091139

Academic Editors: M. Ajmal Khan, Nrup Balar and Pratik Sen

Received: 30 August 2021
Accepted: 13 September 2021
Published: 18 September 2021

1. Introduction

In the past few decades, polymer solar cells (PSCs) have received extensive attention due to their outstanding advantages of high flexibility, low cost, and easy processing [1–5]. For a long time, fullerene-based devices have dominated the development of PSCs [6–8]. In recent years, the emergence of novel narrow bandgap non-fullerene acceptor materials has successfully promoted the power conversion efficiency (PCE) of highly developed PSCs to new heights with records of 18.32% for single-junction [9] and 18.3% for ternary devices [10], showing a bright application prospect.

Morphology optimization is an essential step to improve the PCE of devices. In organic solar cells, additives are effective methods for optimizing the morphology of the active layer and, consequently, the performance of the device [11–15]. For instance, the performance of a classical PSC comprising the donor polymer material polythieno[3,4-b]-thiophene-co-benzodithiophene (PTB7) [16] and the fullerene acceptor [6,6]-phenyl-C_{71}-butyric acid methyl ester ($PC_{71}BM$) can be significantly influenced by the additive of solution. It is found that 1,8-diiodooctane (DIO) additive can effectively inhibit the aggregation of

$PC_{71}BM$ and allow $PC_{71}BM$ to penetrate into the PTB7 phase so that the size of phases can be, thus, optimized [17–21]. Detailed analysis of current density-voltage (*J*–*V*) properties found that the DIO-treated morphology of the active layer can significantly reduce the loss of geminate recombination in PTB7:$PC_{71}BM$ solar cells [22,23]. Although many studies have been carried out regarding the photo-physics properties of PTB7:$PC_{71}BM$ solar cells, many questions are still not clear. For example, the binding energy of excitons in PTB7 and the influence of DIO additives on the carrier recombination dynamics, particularly on the dissociation and recombination dynamics of charge-transfer state (CT) in ultrafast time scale, need to be clarified. The study of these questions is helpful to understand the role of DIO additives in the photoelectric conversion processes of the active layer and has a certain guiding significance for the performance optimization of new polymer photovoltaic devices.

In this work, the effect of DIO additive on the carrier photogeneration and recombination dynamics, as well as device performance of PTB7:$PC_{71}BM$ solar cells, was studied. First, the performances of PTB7:$PC_{71}BM$ solar cells, with and without DIO additive, were examined. It is found that the DIO additive can significantly improve the performance of PTB7:$PC_{71}BM$ devices. In order to understand the photoelectric conversion mechanism behind it, morphology and spectrum studies were carried out. Bias-dependent photoluminescence (PL) of neat PTB7 devices was employed to understand the exciton binding energy of PTB7 excitons. Steady-state and time-resolved PL were employed to understand exciton diffusion and dissociation processes in PTB7:$PC_{71}BM$ devices, and transient absorption (TA) measurements were employed for understanding carrier recombination processes. This work is helpful for understanding the influence of additives on the photoelectric conversion processes of photovoltaic devices.

2. Materials and Methods

2.1. Materials and Fabrication of PSCs

In this work, PTB7 and $PC_{71}BM$ materials were all purchased from the Solarmer Materials Inc. (Beijing, China) without further purification, and the DIO additive was purchased from Sigma-Aldrich (St. Louis, MO, USA). An inverted device configuration was constructed for PTB7:$PC_{71}BM$ solar cells, specifically indium tin oxide (ITO)/ZnO/PTB7:$PC_{71}BM$-/MoO_3/Ag, and the device fabrication process was followed as below. ITO glass substrate was successively cleaned by deionized water, acetone, ethanol, and isopropyl alcohol in an ultrasonic cleaner, and then it was dried in a heat oven for 30 min. ZnO precursor solution was prepared with zinc acetate:2-methoxyethanol:ethanolamine (1 g:10 mL:0.28 mL) for stirring 12 h at 17 °C, and then the ZnO precursor solution was spin-coated (3000 rpm, 30 s) on ITO glass and annealed on a 200 °C hot plate for 1 h to obtain the ZnO electron transport layer. The active layer precursor was a mixed PTB7:$PC_{71}BM$ solution with a mass ratio of 1:1.5 (the concentration of polymer was 9 mg/mL, solvents, chlorobenzene, or chlorobenzene:DIO = 97%:3%, by volume) The active layer precursor was spin-coated on the ZnO layer to get a ~100 nm active layer in a glove box filled with nitrogen. Next, an 8 nm MoO_3 hole transport layer and an 80 nm Ag electrode were successively deposited on the PTB7 or PTB7:$PC_{71}BM$ active layer using a shadow mask to obtain an effective device area of 0.075 cm^2.

2.2. Structure and Steady-state Spectra Measurements

The UV-Vis-NIR spectrometer (Agilent, Cary-5000, Santa Clara, CA, USA) was used to measure the steady-state absorption spectra of neat PTB7 and PTB7:$PC_{71}BM$ blend films. A homemade PL measurement system was used to measure the PL spectra of neat PTB7 and blend PTB7:$PC_{71}BM$ films. The excitation wavelength was 532 nm. The PL signal of sample was collected by two lenses and directed into an optical fiber connected with a spectrometer (Avaspec-ULS2048CL-RS-EVO-UA, Avantes, Apeldoom, The Netherlands). The measured signal was calibrated by a reference light source (Ocean Optics LS-1-CAL, Largo, FL, USA). The bias-dependent PL measurement of the neat PTB7 device was performed by a

spectrometer system equipped with a monochromator (Omni-λ3008i, Zolix, Beijing, China) and a photomultiplier tube (PMTH-S1-CR131A, Zolix, Beijing, China). The bias voltage was provided by a direct current regulated power supply (YB1731A-3A, Lv Yang, Tianjin, China), and the excitation light source was a laser diode emitting at 532 nm. The absorption and PL measurements were carried out at room temperature in air. The atomic force microscopy (AFM, Agilent, AFM-5500, Santa Clara, CA, USA) with tapping mode was used to measure the surface morphology of active layers.

2.3. TA and Time-Resolved Photoluminescence (TRPL) Measurements

The HARPIA-TA (TA—Transient Absorption) spectroscopy system (HARPIA, Light Conversion, Vilnius, Lithuania) described in Refs. [24,25] was employed for TA measurements. The light source of the HARPIA-TA system was a pulsed laser (PHAROS, Light Conversion, Vilnius, Lithuania) emitting at 1030 nm with the repetition rate of 100 kHz and the pulse duration of 190 fs. The light source was divided into two beams. The first beam was used as the pump of an optical parametric amplifier system (OPA, Light Conversion, Vilnius, Lithuania) system, and the output of the OPA was employed for exciting the samples. The second beam was used to generate the probing light (super-continuum white light) of HARPIA-TA system. A mechanical delay stage was employed for adjusting the delay time between the pump and probe pulse.

Time resolved photoluminescence (TRPL) of the pure polymer film and the blended films were measured using a streak camera system described in previous works [26,27]. A fs pulsed laser (Spectra-Physics, Tsunami, Irvine, CA, USA) emitting at 800 nm with 81 MHz and pulse duration of ~100 fs was employed as the light source of the system. The samples were excited by the frequency-doubled light source (400 nm). The PL signal was collected by a lens first (focal length, 50 mm), and it was focused into a spectra meter (Chromex Scientific Ltd, London, the UK) by a second lens. The signal from the spectrometer is collected and detected by a streak camera (Hamamatsu C6860, Sunayama-cho, Japan). The measured TRPL images were conducted background, shading, and spectral sensitivity corrections in sequence. TA and TRPL measurements were conducted at room temperature in air.

3. Results and Discussion

3.1. Steady-State Absorption Properties

Figure 1 shows the absorption spectra of neat PTB7 and PTB7:$PC_{71}BM$ blend films at various treated conditions. The absorption of neat PTB7 film exhibits the main absorption peak at ~677 nm and a shoulder at ~623 nm, which can be assigned to the 0–0 and 0–1 vibronic bands of the transition from S_0 ground state to S_1 excited state, respectively [28]. Moreover, the peak intensity of 0–0 is higher than that of 0–1 vibronic peak, suggesting a significant contribution of J-aggregates in neat PTB7 film [29]. For PTB7:$PC_{71}BM$ blend films, both with and without DIO treatment, there is a strong absorption in the range of 300~750 nm due to the complementary absorption $PC_{71}BM$ for PTB7.

3.2. Morphology and Photovoltaic Properties

The AFM with the tapping mode was employed to characterize surface morphology of the neat PTB7 and PTB7:$PC_{71}BM$ devices without/with DIO treatment, as shown in Figure 2. For neat PTB7 film, the root-mean-square of the surface roughness (S_q) is ~1.12 nm. For the PTB7:$PC_{71}BM$ blend films, S_q of the blend films, without and with DIO additive, are 1.89 nm and 2.86 nm, respectively. Apparently, S_q of the blend films are larger than the neat PTB7 film, which could be attributed to phase separation in the blend films. It should be noted that it is not sufficient to judge the size of phase separation only by AFM data. The reasons are as follows: First, it is difficult to form a "really neat" donor or acceptor phase in the blend film. In many cases, the formed "donor phase" still contains some acceptors inside, and these acceptors will provide D/A interface within the "donor phase" for the exciton dissociation. Second, people cannot distinguish donor or acceptor compositions

from AFM images directly. Sometimes, the observed domain size in AFM image may not reflect the size of separated phases in blend films. We also note that S_q increases after the additive of DIO, suggesting the addition of DIO could adjust surface morphology of PTB7:PC_{71}BM blend films.

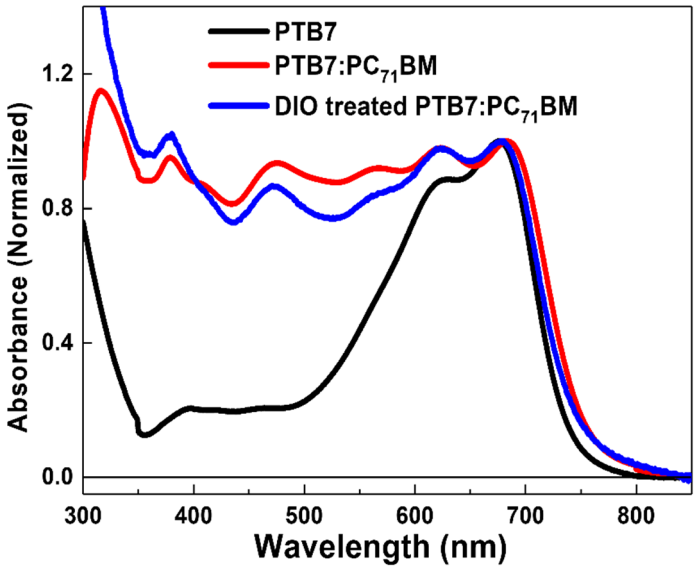

Figure 1. Normalized absorption spectra of neat PTB7 (polythieno[3,4-b]-thiophene-co-benzodithiophene) and PTB7:PC71BM ([6,6]-phenyl-C_{71}-butyric acid methyl ester) blend films with and without DIO (1,8-diiodooctane) additive.

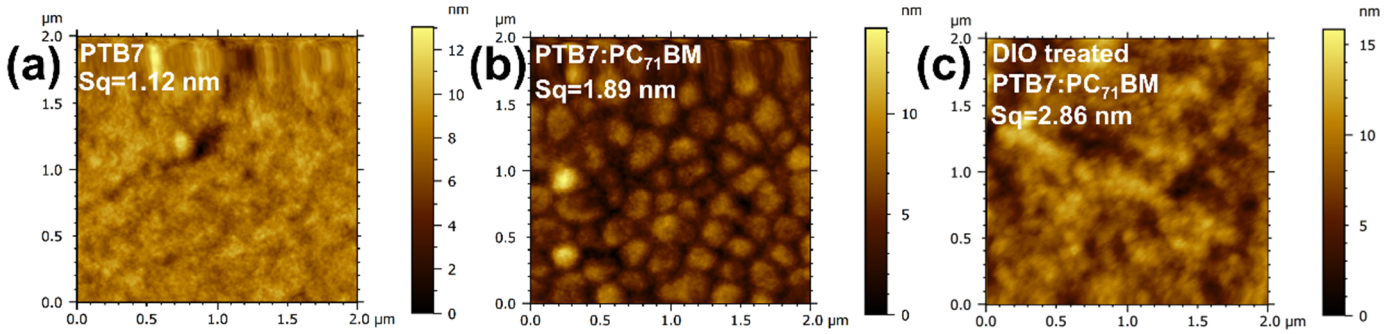

Figure 2. The AFM topographic images of (**a**) neat PTB7 and PTB7:PC_{71}BM blend films (**b**) without and (**c**) with DIO additive.

To examine the influence of DIO additive on the photovoltaic performance of PTB7:-PC_{71}BM solar cells, we measured the *J*–*V* properties of the devices without and with DIO treatment, as shown in Figure 3a. The detailed parameters can be found in Table 1. The PTB7:PC_{71}BM solar cells without DIO processing show an averaged short-circuit current density (J_{sc}) of 11.26 mA/cm^2, open-circuit voltage (V_{oc}) of 0.70 V, fill factor (FF) of 0.46, and PCE of 3.63%. After DIO processing, V_{oc} (from 0.70 V to 0.71 V) does not change much, while J_{sc} (from 11.26 mA/cm^2 to 17.01 mA/cm^2) and FF (from 0.46 to 0.68) increases significantly, resulting in an increased PCE (from 3.63 % to 8.21 %). The external quantum efficiency (EQE) curves of PTB7:PC_{71}BM solar cells are presented in Figure 3b. It can be seen that the EQE of DIO-treated PTB7:PC_{71}BM devices in the wavelength range of 350~750 nm is much higher than that of without DIO additive. We note that the shapes of EQEs in the wavelength range of 350~750 nm are similar to the absorption shapes in Figure 1. This suggests that the excitation of photon energy has a weak influence on the internal charge photogeneration processes of PTB7:PC_{71}BM solar cells in this wavelength range.

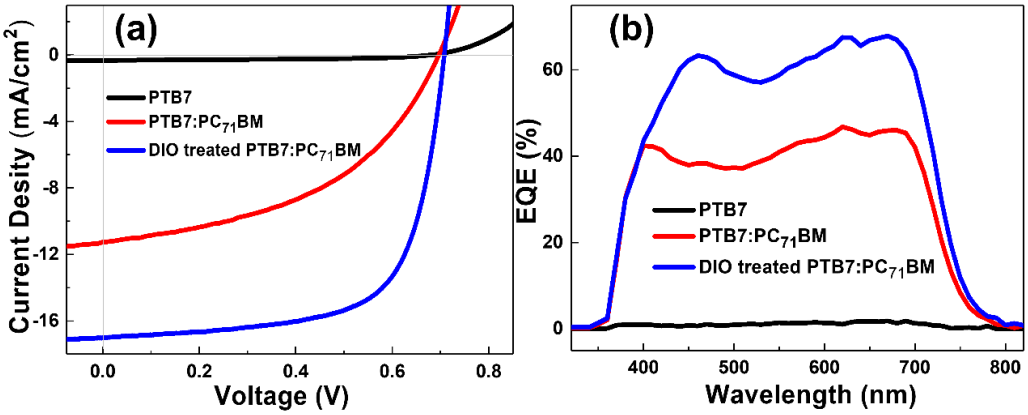

Figure 3. (**a**) The current density-voltage (*J*–*V*) and (**b**) external quantum efficiency (EQE) characteristics of the neat PTB7 and PTB7:$PC_{71}BM$ blend devices without and with DIO treatment.

Table 1. The device parameters of neat PTB7 (polythieno[3,4-b]-thiophene-co-benzodithiophene) and PTB7:PC71BM ([6,6]-phenyl-C_{71}-butyric acid methyl ester) solar cells without/with DIO treatment.

Active Layers	J_{sc} (mA/cm^2)	V_{oc} (V)	*FF*	PCE (%)	PCE_{max} (%)
PTB7	0.32 ± 0.06	0.68 ± 0.02	0.49 ± 0.02	0.11 ± 0.02	0.13
PTB7:$PC_{71}BM$	11.26 ± 0.29	0.70 ± 0.01	0.46 ± 0.01	3.63 ± 0.10	3.73
DIO-treated PTB7:$PC_{71}BM$	17.01 ± 0.25	0.71 ± 0.04	0.68 ± 0.02	8.21 ± 0.15	8.36

3.3. Electric Field Induced Exciton Dissociation

Due to the low dielectric constant and weak intermolecular interactions, the initial photogenerated species in polymeric semiconductors is Frenkel-type exciton, in which the binding energy is usually higher than thermal energy at room temperature [30–32]. Thus, at room temperature, the PTB7 exciton cannot be dissociated effectively, which leads to the low PCE and EQE in pure PTB7 photovoltaic devices, as shown in Figure 3. Since the binding energy of exciton is typically induced by the Coulomb binding energy of the charge pairs [33], the study of electric field-dependent exciton dissociation is helpful to understand the exciton binding energy.

In this work, the bias-dependent PL spectrum of the neat PTB7 device was examined, as shown in Figure 4. It can be seen that the PL intensity of the neat PTB7 device does not change in the bias range of 0 to −2 V, suggesting the electric field of the device under working conditions has a weak influence on the dissociation of PTB7 excitons. To further examine the influence of high electric field on the dissociation of PTB7 excitons, the bias is further increased to −10 V. We observe PL intensity of neat PTB7 device decreases with the increase of bias when the bias is higher than −2 V. When the bias increases to −10 V, the PL intensity decreases to 20% of that at 0 V, suggesting 80% of PTB7 excitons are dissociated. We note that the bias of −10 V corresponds to the electric field of 1.1×10^8 V/m. Assuming this external electric field just overcomes the Coulomb attraction between the positive and negative charge of the charge pairs, a Coulomb binding energy of 0.23 eV can be deduced, see Supporting Information S1. The exciton binding energies of many classical conjugated polymers, such as P3HT (poly(3-hexylthiophene)) and PTB7, has been theoretically studied before. The exciton binding energy of PTB7 was estimated to be varied in the range of 0.22~0.49 eV depending on the constrained values of the dihedral angles, by first-principles calculations [34]. Our estimated value (~0.23 eV) is close to the calculated exciton binding energy of PTB7 at the dihedral angle of 0 (~0.22 eV) in that work. We also noted that the measured exciton binding energy of PTB7 is smaller than that of P3HT (0.28~0.75 eV) studied by theoretical calculations [34–37].

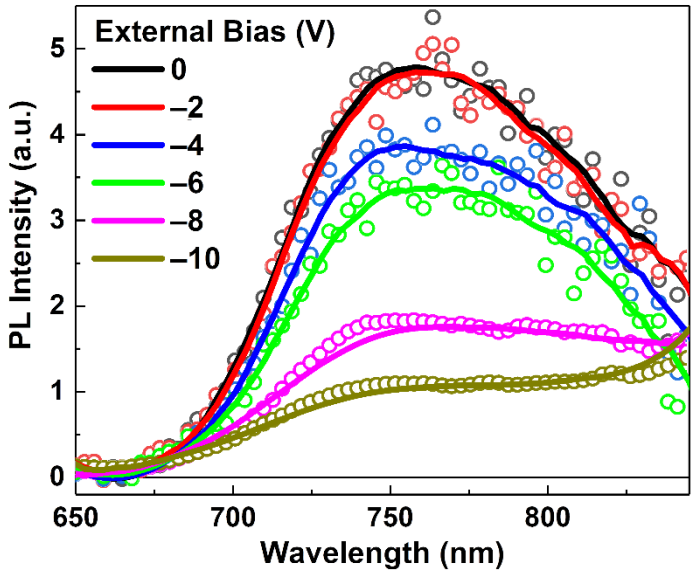

Figure 4. Photoluminescence (PL) spectrum of neat PTB7 device after photoexcitation at 532 nm under various bias electrical field.

3.4. Charge Photogeneration and Recombination Processes

Steady-state PL, TRPL, and TA measurements of neat PTB7 and PTB7:$PC_{71}BM$ devices were performed to further understand the effect of DIO additive on charge photogeneration processes, including the exciton diffusion, dissociation, and recombination processes. The steady-state PL spectra of neat PTB7 and PTB7:$PC_{71}BM$ blend films are shown in Figure 5a. For neat PTB7 film, PL spectrum shows a pronounced emission peak at 770 nm, which originated from the emission of PTB7 excitons. For the PTB7:$PC_{71}BM$ blend films, an additional PL peak at ~715 nm appears beyond the ~770 nm peak and can be attributed to the emission of $PC_{71}BM$ in the blend films.

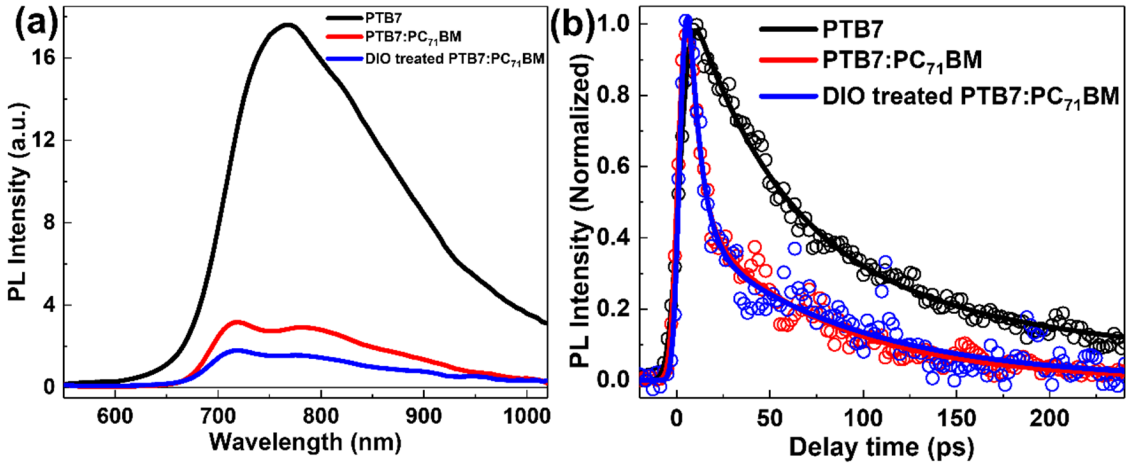

Figure 5. (**a**) Steady-state PL spectra and (**b**) TRPL (time resolved photoluminescence) kinetics of neat PTB7 and PTB7:$PC_{71}BM$ blend films at the indicated preparation conditions. The excitation wavelengths for steady-state PL and TRPL measurements were 532 nm and 400 nm, respectively. TRPL kinetics were probed at 780 nm with an excitation fluency of ~4×10^{10} photons·cm^{-2}·$pulse^{-1}$. The solid lines in (**b**) are fitting curves using double exponential decay functions.

In general, the PL quenching efficiency (ΔPL) can not only reflect the exciton diffusion and dissociation efficiency of neat donor (acceptor) excitons but also gives insight into the average domain size and miscibility of the blend phase [38]. In this work, the ΔPL of PTB7 exciton was estimated by comparing the PL intensity of PTB7:$PC_{71}BM$ blend films with that of neat PTB7 film. The ΔPL of PTB7 are 84.3% and 91.1% for PTB7:$PC_{71}BM$ films

without and with DIO additive, respectively. The increased ΔPL of PTB7 exciton with DIO additive suggests that DIO additive can improve the dissociation efficiency of PTB7 in the blend film. Besides, we note that PL intensity of $PC_{71}BM$ in PTB7:$PC_{71}BM$ film with DIO additive is much lower than that without DIO additive, suggesting the exciton dissociation of $PC_{71}BM$ in the blend film is also increased after the addition of DIO. In PSCs, the exciton dissociation efficiency depends on the exciton diffusion coefficient and the lifetime of neat donor (or acceptor) film, on the one hand, and the phase separation scale of donor (or acceptor) phase in the blend film, on the other hand [39]. Assuming the exciton diffusion coefficient and a lifetime of neat donor (or acceptor) film are the same with and without DIO additive, the increased ΔPL of PTB7 and $PC_{71}BM$ excitons in the blend film with DIO additive suggests that DIO additive can improve the miscibility between PTB7 and $PC_{71}BM$ materials. In other words, the addition of DIO reduces the phase scales of both donor and acceptor in PTB7:$PC_{71}BM$ film, resulting in a higher exciton dissociation efficiency.

Figure 5b shows the normalized TRPL kinetics of neat PTB7 and PTB7:$PC_{71}BM$ blend films after photo-excitation at 400 nm and probing at 780 nm. It can be seen that TRPL kinetics of blend films decay much faster than that of neat PTB7 kinetics, suggesting the PTB7 excitons dissociate efficiently at the interface after blending with the $PC_{71}BM$ acceptor material. Meanwhile, we note that all the blend films exhibit double exponential decay behaviors, that a fast decay component within the instrumental function and a slower decay component. This indicates the dissociation of excitons are not uniform in the blend films. The non-uniform exciton dissociation may originate from two aspects: one is the heterogeneity of donor (acceptor) phase size, and the other is the contribution of both donor and acceptor excitons. We also note that normalized TRPL kinetics of the blend films with and without DIO treatment are similar, which usually leads to similar steady-state PL intensity of both types of blend films. However, an obvious difference in steady-state PL intensity for these two types of blend films was observed in that the PL intensity of the blend film without DIO treatment is stronger than that of with DIO treatment, as shown in Figure 5a. This strongly suggests there are exciton quenching processes faster than the TRPL instrument response function in both blend films, and these ultrafast exciton quenching processes lead to the pronounced difference of PL intensity in both types of blend films.

The TA measurement of PTB7:$PC_{71}BM$ blend films was employed to understand the carrier photogeneration and recombination processes. Figure 6 shows the representative TA spectrum of the DIO-treated PTB7:$PC_{71}BM$ device at various delay times under the excitation wavelength of 600 nm, which can excite the PTB7 phase in the blend film predominately. It can be seen that the spectrum shows two negative peaks located at ~627 nm and ~677 nm, showing similar characteristics of the steady-state absorption spectrum of PTB7 (see Figure 1), and can, thus, be attributed to ground state bleaching of PTB7 in the blend films. Furthermore, TA spectra of without/with DIO-treated devices both show a wide positive absorption band at 740~900 nm in the measured wavelength range, which can be attributed to the absorption of excited-state populations. Similar TA spectrum properties were observed in the blend films without DIO additive, as shown in Supporting Information Figure S1 (see Supplementary Materials).

To examine the carrier recombination mechanism in PTB7:$PC_{71}BM$ films, we examined TA bleaching kinetics under various excitation fluencies, as shown in Figure 7. It can be seen that all the kinetics show a fast decay at the early timescale and a slow decay at a longer timescale. The fast decay component can be affected by many photoexcited processes, such as exciton diffusion and dissociation, charge photogeneration, and recombination, while the slow decay component is mainly affected by carrier recombination [39]. In PSCs, geminate and bimolecular recombination are the two dominant carrier recombination forms. Geminate recombination is typically induced by the recombination of charge pair origin from the same absorbed photon, while bimolecular recombination is induced by the charges generated from different photons. Accordingly, geminate and bimolecular recombination processes are independent and dependent with excitation fluency, respec-

tively [30]. We find the slower decay of the kinetics under excitation fluencies of 1.16×10^{13} to 3.05×10^{13} photon·cm^{-2}·pulse^{-1} are similar in both types of the blend films (as shown in Figure 7a,b), suggesting carrier recombination of both blend films in the ultrafast time scale is independent with carrier concentration. In other words, carrier recombination in the blend films with and without DIO additive are dominated by geminate recombination in the ultrafast timescale. By comparing TA kinetics of the blend films under the same excitation fluency, we find that lifetime of the PTB7:PC_{71}BM device without DIO treatment is ~8 ns, which is significantly faster than that of with DIO processing (~25 ns) (see Supporting Information Table S1). This notably prolonged decay time indicates that the DIO additive processing can effectively suppress the germinate recombination in PTB7:PC_{71}BM device.

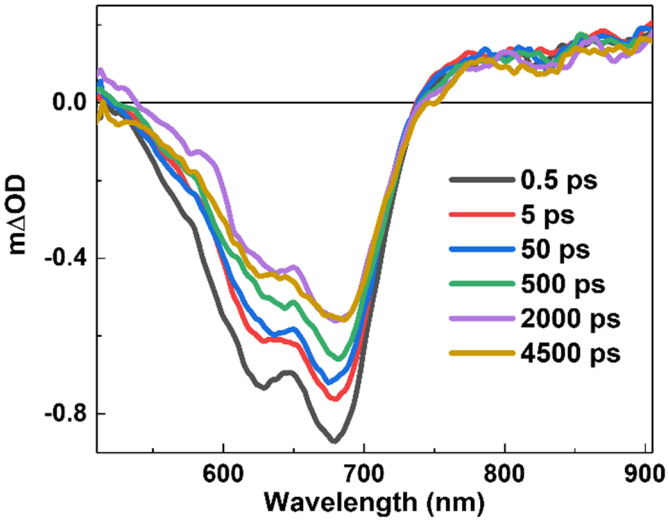

Figure 6. The representive TA (transient absorption) spectrum of DIO-treated PTB7:PC_{71}BM film at indicated delay times under the 600 nm light excitation with an excitation fluency of 1.16×10^{13} photon·cm^{-2}·pulse^{-1}.

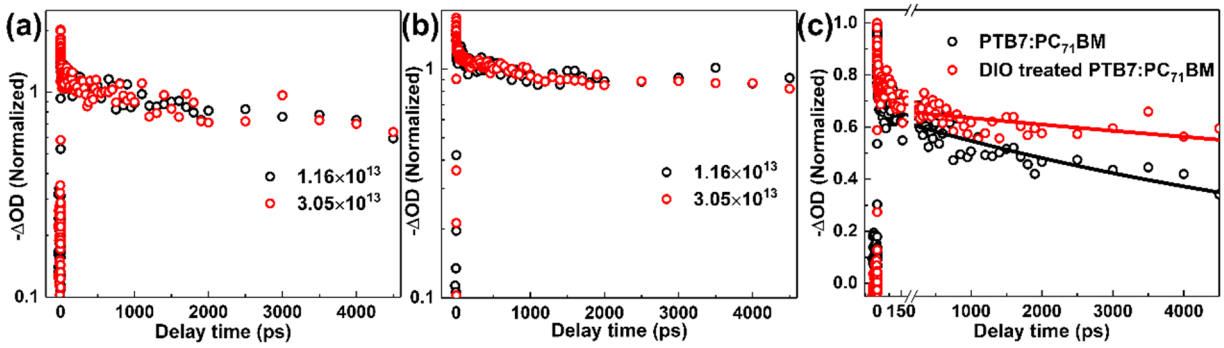

Figure 7. Normalized TA bleaching kinetics of PTB7:PC_{71}BM blend films (**a**) without and (**b**) with DIO additive at 677 nm after photoexcitation at 600 nm under various photoexcitation fluencies (1.16×10^{13} and 3.05×10^{13} photon·cm^{-2}·pulse^{-1}). (**c**) Normalized TA bleaching kinetics of PTB7:PC_{71}BM blend films without and with DIO additive under an excitation fluency of 1.16×10^{13} photon·cm^{-2}·pulse^{-1}. The solid lines are fitting curves by using single exponential decay functions.

Considering the morphology information (see Figure 2) and the exciton dissociation process (see Figure 5), we can infer that the increased exciton dissociation efficiency and suppressed CT recombination of the DIO-treated device play an important role to attain a higher short-circuit current and, thus, the PCE of PTB7:PC_{71}BM solar cells. However, we cannot completely rule out the possible influence of non-geminate recombination on the device performance because we did not examine the carrier dynamics on a longer time scale (ns~ms) in this work. It has been shown that non-Langevin bimolecular recombination

can be suppressed in PTB7:$PC_{71}BM$ devices [40], so it is plausible that the DIO treatment would also influence the non-geminate recombination behavior.

4. Conclusions

In this work, the effect of DIO additive on the carrier photogeneration dynamics, as well as device performance of PTB7:$PC_{71}BM$ solar cells, has been studied. We found that the excitons cannot be dissociated by the electric field under working conditions but can be effectively dissociated by the high electric field. We find that the DIO additive reduces the phase size of PTB7 in the blend film, resulting in an increasing exciton dissociation efficiency. Besides, DIO additive suppresses geminate carrier recombination in PTB7:$PC_{71}BM$ devices on the ultrafast time scale. The increased exciton dissociation efficiency and suppressed carrier recombination play an important role for DIO-treated film to obtain a higher J_{sc} and, consequently, the PCE of PTB7:$PC_{71}BM$ solar cells.

Supplementary Materials: The following are available online at https://www.mdpi.com/article/10.3390/cryst11091139/s1, Figure S1: TA spectrum of PTB7:$PC_{71}BM$ film without DIO treatment at indicated delay times after 600 nm excitation with an excitation fluency of 1.16×10^{13} photon·cm^{-2}·$pulse^{-1}$, Table S1: Fitting parameters of TA kinetics traces in Figure 7c. Reference [41] is cited in supplementary materials.

Author Contributions: Conceptualization, W.Z.; Data curation, X.S., R.H., G.W., X.Z., M.Q. and X.H.; Formal analysis, G.W. and J.P.; Funding acquisition, R.H., G.W. and W.Z.; Investigation, X.S., R.H., G.W., X.Z., M.Q. and X.H.; Methodology, R.H. and W.Z.; Supervision, W.Z.; Writing—original draft, G.W.; Writing—review and editing, X.S., R.H., X.Z., M.Q. and W.Z. All authors have read and agreed to the published version of the manuscript.

Funding: This work was supported by the funding from Natural Science Foundation of China (Grant No. 21903017, 21603020), Guangzhou Science and Technology Planning Project (202102010443), Young Talents Program of Guangzhou University (Grant No. RQ2020080), Science and Technology Research Program of Chongqing Municipal Education Commission (Grant No. KJQN201901319, KJQN202001323), and Innovation Research for the Postgraduates of Guangzhou University (Grant No. 2020GDJC-M50).

Institutional Review Board Statement: Not Applicable.

Informed Consent Statement: Not Applicable.

Data Availability Statement: The data presented in this study are available on request from the corresponding author.

Acknowledgments: The authors acknowledge the funding supports from institutes of Natural Science Foundation of China, Guangzhou Science and Technology Bureau, Chongqing Municipal Education Commission and Guangzhou University.

Conflicts of Interest: The authors declare that they have no known competing financial interests or personal relationships that could have appeared to influence the work reported in this paper.

References

1. Hou, J.; Inganäs, O.; Friend, R.H.; Gao, F. Organic solar cells based on non-fullerene acceptors. *Nat. Mater.* **2018**, *17*, 119–128. [CrossRef]
2. Liu, S.; Yuan, J.; Deng, W.; Luo, M.; Xie, Y.; Liang, Q.; Zou, Y.; He, Z.; Wu, H.; Cao, Y. High-efficiency organic solar cells with low non-radiative recombination loss and low energetic disorder. *Nat. Photonics* **2020**, *14*, 300–305. [CrossRef]
3. Qi, F.; Jiang, K.; Lin, F.; Wu, Z.; Zhang, H.; Gao, W.; Li, Y.; Cai, Z.; Woo, H.Y.; Zhu, Z.; et al. Over 17% Efficiency binary organic solar cells with photoresponses reaching 1000 nm enabled by selenophene-fused nonfullerene acceptors. *ACS Energy Lett.* **2020**, *6*, 9–15. [CrossRef]
4. Zhu, L.; Zhang, M.; Zhou, G.; Hao, T.; Xu, J.; Wang, J.; Qiu, C.; Prine, N.; Ali, J.; Feng, W.; et al. Efficient organic solar cell with 16.88% efficiency enabled by refined acceptor crystallization and morphology with improved charge transfer and transport properties. *Adv. Energy Mater.* **2020**, *10*, 1904234. [CrossRef]
5. Cui, Y.; Yao, H.; Hong, L.; Zhang, T.; Tang, Y.; Lin, B.; Xian, K.; Gao, B.; An, C.; Bi, P.; et al. Organic photovoltaic cell with 17% efficiency and superior processability. *Natl. Sci. Rev.* **2019**, *7*, 1239–1246. [CrossRef]

6. Li, Z.; Yang, D.; Zhao, X.; Zhang, T.; Zhang, J.; Yang, X. Achieving an efficiency exceeding 10% for fullerene-based polymer solar cells employing a thick active layer via tuning molecular weight. *Adv. Funct. Mater.* **2017**, *28*, 1705257. [CrossRef]
7. Dennler, G.; Scharber, M.C.; Brabec, C.J. Polymer-fullerene bulk-heterojunction solar cells. *Adv. Mater.* **2009**, *21*, 1323–1338. [CrossRef]
8. Vandewal, K.; Gadisa, A.; Oosterbaan, W.; Bertho, S.; Banishoeib, F.; Van Severen, I.; Lutsen, L.; Cleij, T.; Vanderzande, D.; Manca, J.V. The relation between open-circuit voltage and the onset of photocurrent generation by charge-transfer absorption in polymer: Fullerene bulk heterojunction solar cells. *Adv. Funct. Mater.* **2008**, *18*, 2064–2070. [CrossRef]
9. Li, C.; Zhou, J.; Song, J.; Xu, J.; Zhang, H.; Zhang, X.; Guo, J.; Zhu, L.; Wei, D.; Han, G.; et al. Non-fullerene acceptors with branched side chains and improved molecular packing to exceed 18% efficiency in organic solar cells. *Nat. Energy* **2021**, *6*, 605–613. [CrossRef]
10. Lin, Y.B.; Nugraha, M.I.; Firdaus, Y.; Scaccabarozzi, A.D.; Aniés, F.; Emwas, A.-H.; Yengel, E.; Zheng, X.; Liu, J.; Wahyudi, W.; et al. A simple n-dopant derived from diquat boosts the efficiency of organic solar cells to 18.3%. *ACS Energy Lett.* **2020**, *5*, 3663–3671. [CrossRef]
11. Zhang, Q.; Bao, C.; Cui, S.; Zhong, P.; Zhang, K.; Zhu, W.; Liu, Y. Boosting the efficiency of PTB7-Th:$PC_{71}BM$ polymer solar cells via a low-cost halogen-free supramolecular solid additive. *J. Mater. Chem. C* **2020**, *8*, 16551–16560. [CrossRef]
12. Liu, X.; Ma, R.; Wang, Y.; Du, S.; Tong, J.; Shi, X.; Li, J.; Bao, X.; Xia, Y.; Liu, T.; et al. Significantly boosting efficiency of polymer solar cells by employing a nontoxic halogen-free additive. *ACS Appl. Mater. Interfaces* **2021**, *13*, 11117–11124. [CrossRef] [PubMed]
13. Kong, J.; Hwang, I.-W.; Lee, K. Top-down approach for nanophase reconstruction in bulk heterojunction solar cells. *Adv. Mater.* **2014**, *26*, 6275–6283. [CrossRef]
14. Zhang, L.; Lin, B.; Hu, B.; Xu, X.; Ma, W. Blade-cast nonfullerene organic solar cells in air with excellent morphology, efficiency, and stability. *Adv. Mater.* **2018**, *30*, 1800343. [CrossRef] [PubMed]
15. Kim, W.; Kim, J.K.; Kim, E.; Ahn, T.K.; Wang, D.H.; Park, J.H. Conflicted effects of a solvent additive on PTB7:$PC_{71}BM$ bulk heterojunction solar cells. *J. Phys. Chem. C* **2015**, *119*, 5954–5961. [CrossRef]
16. Liang, Y.; Xu, Z.; Xia, J.; Tsai, S.-T.; Wu, Y.; Li, G.; Ray, C.; Yu, L. For the bright future-bulk heterojunction polymer solar cells with power conversion efficiency of 7.4%. *Adv. Mater.* **2010**, *22*, E135–E138. [CrossRef] [PubMed]
17. Chen, W.; Xu, T.; He, F.; Wang, W.; Wang, C.; Strzalka, J.; Liu, Y.; Wen, J.; Miller, D.J.; Chen, J.; et al. Hierarchical nano-morphologies promote exciton dissociation in polymer/fullerene bulk heterojunction solar cells. *Nano Lett.* **2011**, *11*, 3707–3713. [CrossRef] [PubMed]
18. Liu, F.; Zhao, W.; Tumbleston, J.R.; Wang, C.; Gu, Y.; Wang, D.; Briseno, A.L.; Ade, H.; Russell, T.P. Understanding the morphology of PTB7:PCBM Blends in organic photovoltaics. *Adv. Energy Mater.* **2013**, *4*, 1301377. [CrossRef]
19. Hammond, M.R.; Kline, R.J.; Herzing, A.A.; Richter, L.J.; Germack, D.S.; Ro, H.-W.; Soles, C.L.; Fischer, D.A.; Xu, T.; Yu, L.; et al. Molecular order in high-efficiency polymer/fullerene bulk heterojunction solar cells. *ACS Nano* **2011**, *5*, 8248–8257. [CrossRef] [PubMed]
20. Lu, L.; Yu, L. Understanding low bandgap polymer PTB7 and optimizing polymer solar cells based on it. *Adv. Mater.* **2014**, *26*, 4413–4430. [CrossRef]
21. Supasai, T.; Amornkitbamrung, V.; Thanachayanont, C.; Tang, I.-M.; Sutthibutpong, T.; Rujisamphan, N. Visualizing nanoscale phase morphology for understanding photovoltaic performance of PTB7: $PC_{71}BM$ solar cell. *Appl. Surf. Sci.* **2017**, *422*, 509–517. [CrossRef]
22. Foertig, A.; Kniepert, J.; Gluecker, M.; Brenner, T.; Dyakonov, V.; Neher, D.; Deibel, C. Nongeminate and geminate recombi-nation in PTB7:$PC_{71}BM$ solar cells. *Adv. Funct. Mater.* **2014**, *24*, 1306–1311. [CrossRef]
23. Kniepert, J.; Lange, I.; Heidbrink, J.; Kurpiers, J.; Brenner, T.J.K.; Koster, L.J.A.; Neher, D. Effect of solvent additive on generation, recombination, and extraction in PTB7:PCBM solar cells: A conclusive experimental and numerical simulation study. *J. Phys. Chem. C* **2015**, *119*, 8310–8320. [CrossRef]
24. Wen, G.; Hu, R.; Su, X.; Chen, Z.; Zhang, C.; Peng, J.; Zou, X.; He, X.; Dong, G.; Zhang, W. Excited-state properties of Y-series small molecule semiconductors. *Dye. Pigm.* **2021**, *192*, 109431. [CrossRef]
25. Wen, G.; Zou, X.; Hu, R.; Peng, J.; Chen, Z.; He, X.; Dong, G.; Zhang, W. Ground- and excited-state characteristics in photo-voltaic polymer N2200. *RSC Adv.* **2021**, *11*, 20191–20199. [CrossRef]
26. Su, X.; Zeng, X.; Nemec, H.; Zou, X.; Zhang, W.; Borgström, M.T.; Yartsev, A. Effect of hydrogen chloride etching on carrier recombination processes of indium phosphide nanowires. *Nanoscale* **2019**, *11*, 18550–18558. [CrossRef] [PubMed]
27. Zou, X.; Li, C.; Su, X.; Liu, Y.; Finkelstein-Shapiro, D.; Zhang, W.; Yartsev, A. Carrier recombination processes in GaAs wafers passivated by wet nitridation. *ACS Appl. Mater. Interfaces* **2020**, *12*, 28360–28367. [CrossRef] [PubMed]
28. Bencheikh, F.; Duché, D.; Ruiz, C.M.; Simon, J.-J.; Escoubas, L. Study of optical properties and molecular aggregation of con-jugated low band gap copolymers: PTB7 and PTB7-Th. *J. Phys. Chem. C* **2015**, *119*, 24643–24648. [CrossRef]
29. Más-Montoya, M.; Janssen, R.A.J. The effect of H- and J-aggregation on the photophysical and photovoltaic properties of small thiophene-pyridine-DPP molecules for bulk-heterojunction solar cells. *Adv. Funct. Mater.* **2017**, *27*, 1605779. [CrossRef]
30. Clarke, T.M.; Durrant, J.R. Charge photogeneration in organic solar cells. *Chem. Rev.* **2010**, *110*, 6736–6767. [CrossRef]
31. Hedley, G.J.; Ruseckas, A.; Samuel, I.D.W. Light harvesting for organic photovoltaics. *Chem. Rev.* **2016**, *117*, 796–837. [CrossRef]
32. Wang, R.; Zhang, C.; Li, Q.; Zhang, Z.; Wang, X.; Xiao, M. Charge separation from an intra-moiety intermediate state in the high-performance PM6:Y6 organic photovoltaic blend. *J. Am. Chem. Soc.* **2020**, *142*, 12751–12759. [CrossRef]

33. Xie, Y.; Wu, H. Balancing charge generation and voltage loss toward efficient nonfullerene organic solar cells. *Mater. Today Adv.* **2020**, *5*, 100048. [CrossRef]
34. Bhatta, R.S.; Tsige, M. Chain length and torsional dependence of exciton binding energies in P3HT and PTB7 conjugated polymers: A first-principles study. *Polymer* **2014**, *55*, 2667–2672. [CrossRef]
35. Dkhissi, A. Excitons in organic semiconductors. *Synth. Met.* **2011**, *161*, 1441–1443. [CrossRef]
36. Zhu, L.; Yi, Y.; Chen, L.; Shuai, Z. Exciton binding energy of electronic polymers: A first principles study. *J. Theor. Comput. Chem.* **2008**, *7*, 517–530. [CrossRef]
37. Deibel, C.; Mack, D.; Gorenflot, J.; Schöll, A.; Krause, S.; Reinert, F.; Rauh, D.; Dyakonov, V. Energetics of excited states in the conjugated polymer poly(3-hexylthiophene). *Phys. Rev. B* **2010**, *81*, 085202. [CrossRef]
38. Ma, M.; Ji, Q.; Yin, L.; Lin, K.; Wen, G.; Xu, Y.; Zhang, N.; Dong, G.; Yu, L.; Zhang, W.; et al. Core unit engineering of star-shaped acceptor polymers for all-polymer solar cells. *Sol. Energy* **2020**, *207*, 199–208. [CrossRef]
39. Zhang, W.; Hu, R.; Zeng, X.; Su, X.; Chen, Z.; Zou, X.; Peng, J.; Zhang, C.; Yartsev, A. Effect of post-thermal annealing on the performance and charge photogeneration dynamics of PffBT4T-2OD/$PC_{71}BM$ solar cells. *Polymers* **2019**, *11*, 408. [CrossRef] [PubMed]
40. Stolterfoht, M.; Philippa, B.; Armin, A.; Pandey, A.K.; White, R.D.; Burn, P.L.; Meredith, P.; Pivrikas, A. Advantage of sup-pressed non-langevin recombination in low mobility organic solar cells. *Appl. Phys. Lett.* **2014**, *105*, 013302. [CrossRef]
41. Hughes, M.P.; Rosenthal, K.D.; Ran, N.A.; Seifrid, M.; Bazan, G.C.; Nguyen, T.-Q. Determining the dielectric constants of organic photovoltaic materials using impedance spectroscopy. *Adv. Funct. Mater.* **2018**, *28*, 1801542. [CrossRef]